ANNEX I: DADES METEOROLÒGIQUES METEONORM

TFM
Nombre del sitio

42.434
Latitud [°N]

1.551
Longitud [°E]

2189
Altitud [msnm]

III, 2
Región climática

Estándar
Modelo irradiancia

Estándar
Modelo temperatura

Perez
Modelo irrad. incl.

2000–2009
Periodo de temperatura

1991–2010
Periodo de radiación

Preconfigurado
Horizonte

Información adicional

Incertidumbre de valores anuales: Gh = 4%, Bn = 7%, Gk = 4%, Ta = 2,3 °C
Tendencia de gh / década: -
Variabilidad de gh / año: 2,7%
Sitios de radiación interpolados: Datos de satélite (Parte de los datos de satélite: 100%)
Temperature interpolation locations: MOUNT AIGOUAL (AUT) (248 km), Burgos/Villafria (425 km), Logrono/Agoncillo (319 km), LEON/VIRGEN CAMINO (590 km), PAMPLONA/NOAIN (263 km), CAPE BEAR (130 km)
P10 and P90 of yearly Gh, referenced to average: 96,2%, 103,2%

Mes	**G_Ghhor**	**G_Dhhor**	**Ta**	**FF**
	[W/m2]	[W/m2]	[°C]	[m/s]
Enero	91	33	-3.5	6.4
Febrero	127	42	-2.9	6.5
Marzo	176	63	-0.3	6.6
Abril	212	102	1.9	6.3
Mayo	245	99	6.2	5.6
Junio	287	101	11.1	5.5
Julio	312	98	12.5	5.5
Agosto	269	88	12.4	5.4
Setiembre	210	71	8.8	5.3
Octubre	143	57	5.1	5.7
Noviembre	102	36	-0.3	6.4
Diciembre	80	29	-3.1	6.3
Año	188	68	4.0	6.0

Ta: Temperatura del aire
FF: Velocidad del viento
G_Ghhor: Irradiancia media de la radiacion global horizontal, con horizonte elevado
G_Dhhor: Irradiancia media de la radiacion difusa horizontal, con horizonte elevado

Radiación mensual

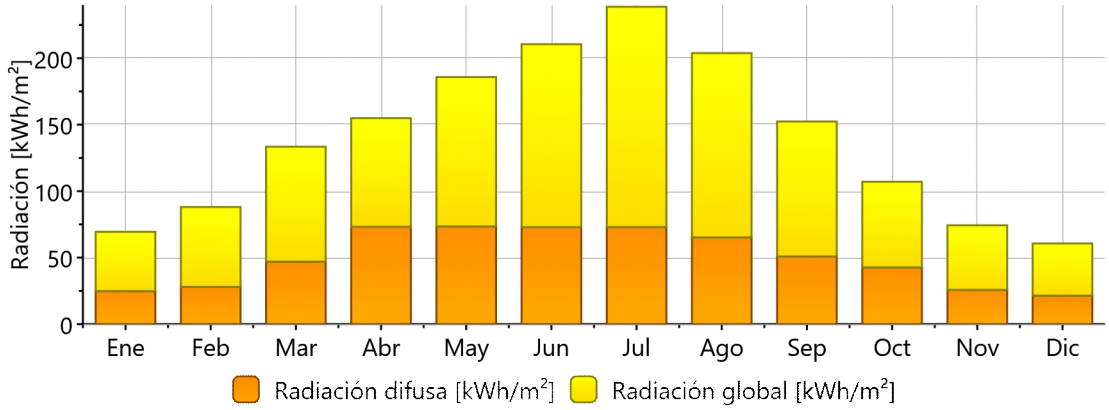

Radiación global diaria

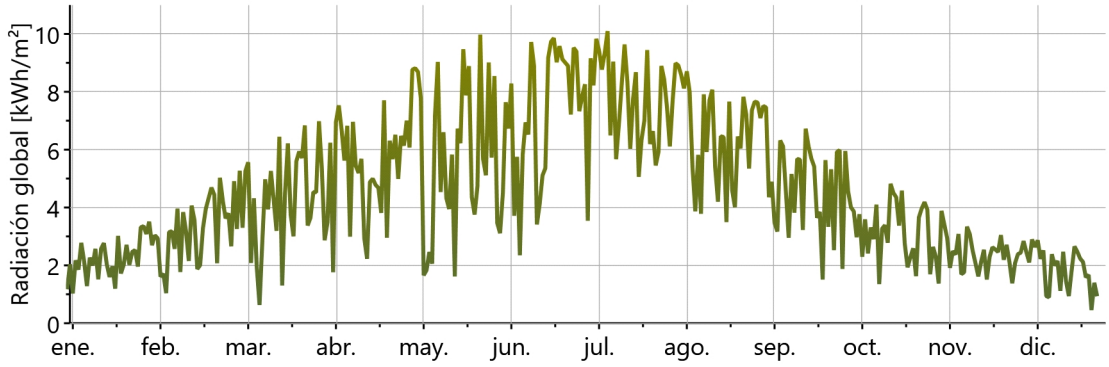

Temperatura mensual

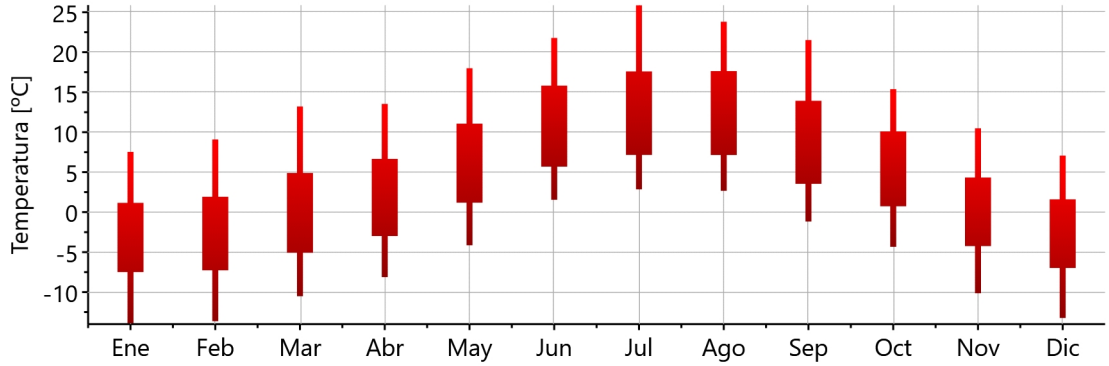

Temperatura diaria

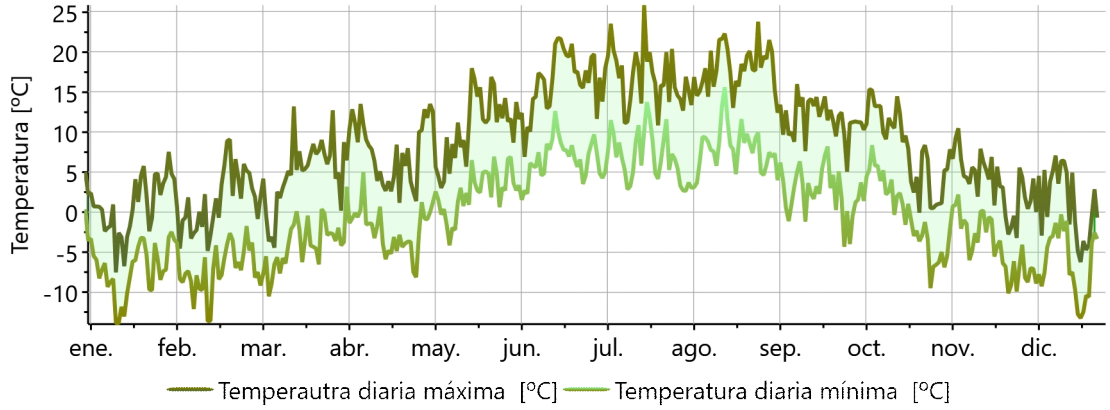

Precipitación

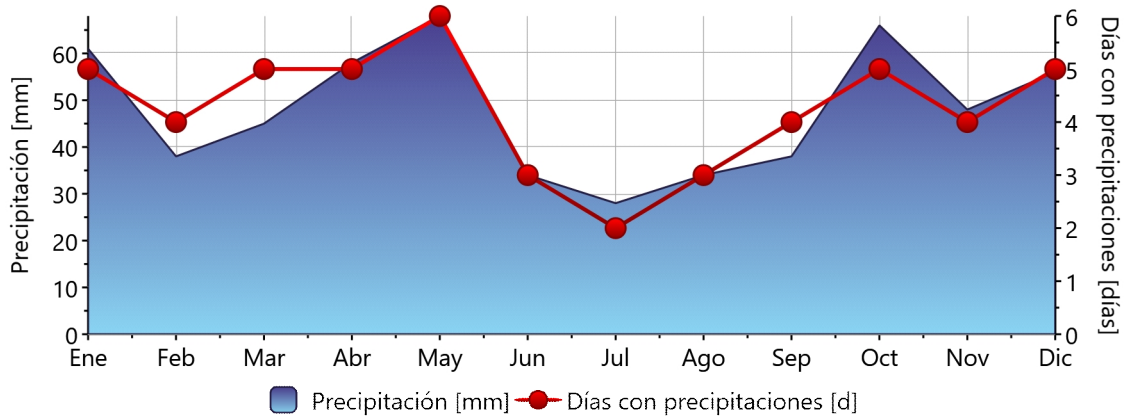

Duración de la insolación

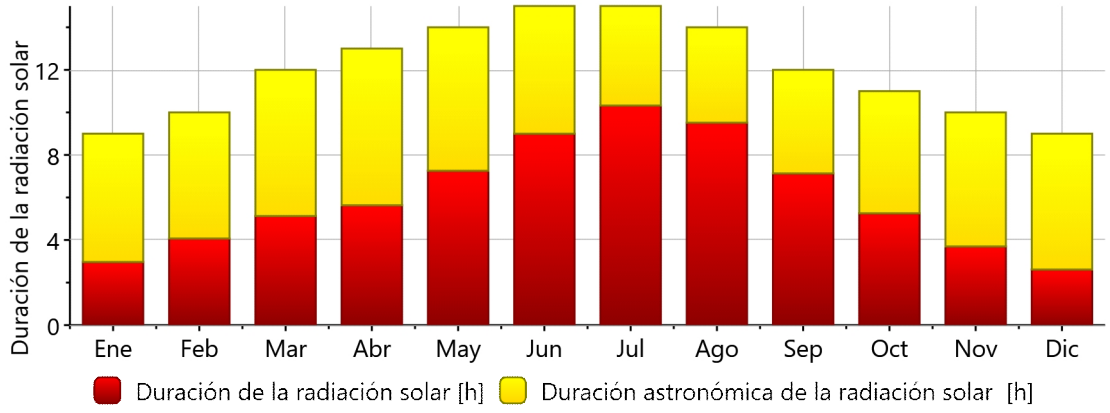

Horizonte

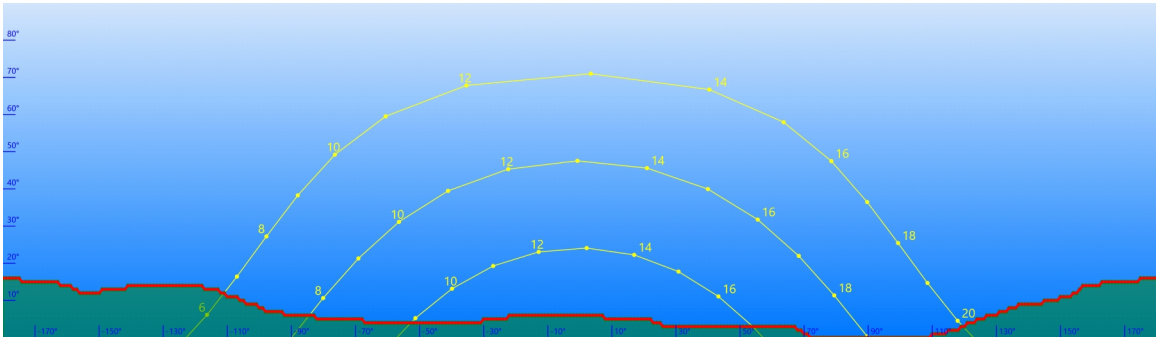

Horizonte final

Camino solar

Horizon filename: C:\Users\Origina\Documents\dtmh_42.434_1.551.hor

ANNEX II: FITXA TÈCNICA SUNPOWER SPR-X21-345

SunPower® X-Series Residential Solar Panels | X21-335-BLK | X21-345

More than 21% Efficiency

Ideal for roofs where space is at a premium or where future expansion might be needed.

Maximum Performance

Designed to deliver the most energy in demanding real-world conditions, in partial shade and hot rooftop temperatures.[1,2,4]

Premium Aesthetics

SunPower® Signature™ Black X-Series panels blend harmoniously into your roof. The most elegant choice for your home.

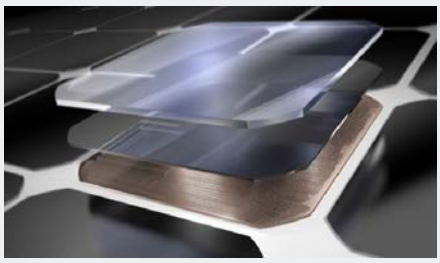

Maxeon® Solar Cells: Fundamentally better
Engineered for performance, designed for durability.

Engineered for Peace of Mind

Designed to deliver consistent, trouble-free energy over a very long lifetime. [3,4]

Designed for Durability

The SunPower Maxeon Solar Cell is the only cell built on a solid copper foundation. Virtually impervious to the corrosion and cracking that degrade conventional panels. [3]

Same excellent durability as E-Series panels.
#1 Rank in Fraunhofer durability test.[9]
100% power maintained in Atlas 25+ comprehensive durability test.[10]

Unmatched Performance, Reliability & Aesthetics

SIGNATURE™ BLACK
SPR-X21-335-BLK

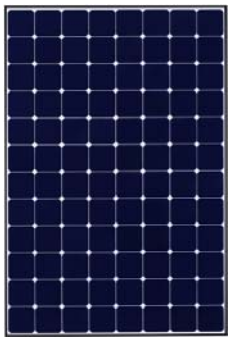

SPR-X21-345

X21 SERIES

Highest Efficiency[5]

Generate more energy per square foot

X-Series residential panels convert more sunlight to electricity by producing 38% more power per panel[1] and 70% more energy per square foot over 25 years.[1,2,3]

Highest Energy Production[6]

Produce more energy per rated watt

High year-one performance delivers 8–10% more energy per rated watt.[2] This advantage increases over time, producing 21% more energy over the first 25 years to meet your needs.[3]

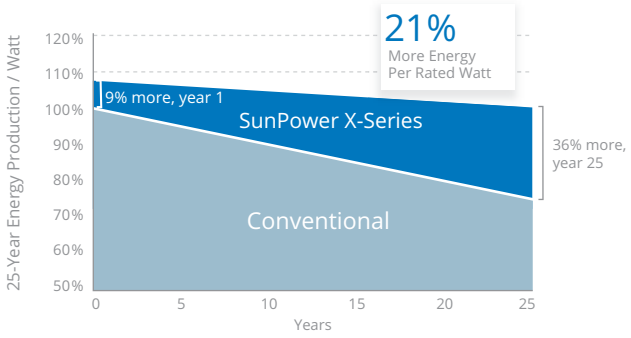

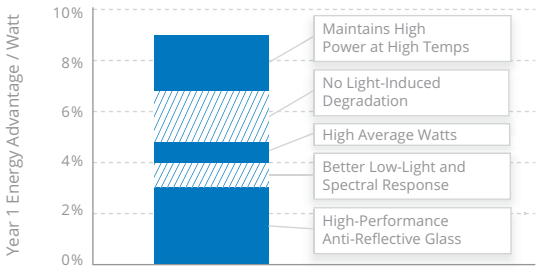

SUNPOWER®

SunPower® X-Series Residential Solar Panels | X21-335-BLK | X21-345

SunPower Offers The Best Combined Power And Product Warranty

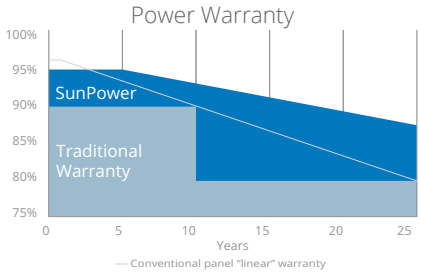

More guaranteed power: 95% for first 5 years, –0.4%/yr. to year 25 [7]

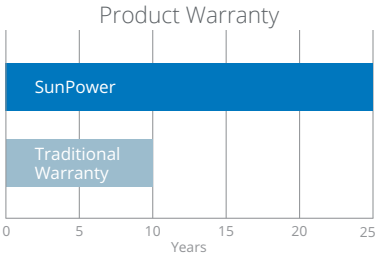

Combined Power and Product defect 25-year coverage [8]

Electrical Data		
	SPR-X21-335-BLK	SPR-X21-345
Nominal Power (Pnom)[11]	335 W	345 W
Power Tolerance	+5/–0%	+5/–0%
Avg. Panel Efficiency[12]	21.0%	21.5%
Rated Voltage (Vmpp)	57.3 V	57.3 V
Rated Current (Impp)	5.85 A	6.02 A
Open-Circuit Voltage (Voc)	67.9 V	68.2 V
Short-Circuit Current (Isc)	6.23 A	6.39 A
Max. System Voltage	600 V UL & 1000 V IEC	
Maximum Series Fuse	15 A	
Power Temp Coef.	–0.29% / ° C	
Voltage Temp Coef.	–167.4 mV / ° C	
Current Temp Coef.	2.9 mA / ° C	

Tests And Certifications	
Standard Tests[13]	UL1703 (Type 2 Fire Rating), IEC 61215, IEC 61730
Quality Certs	ISO 9001:2008, ISO 14001:2004
EHS Compliance	RoHS, OHSAS 18001:2007, lead free, REACH SVHC-163, PV Cycle
Sustainability	Cradle to Cradle Certified™ Silver (eligible for LEED points)[14]
Ammonia Test	IEC 62716
Desert Test	10.1109/PVSC.2013.6744437
Salt Spray Test	IEC 61701 (maximum severity)
PID Test	Potential-Induced Degradation free: 1000 V[9]
Available Listings	UL, TUV, JET, MCS, CSA, FSEC, CEC

Operating Condition And Mechanical Data	
Temperature	–40° F to +185° F (–40° C to +85° C)
Impact Resistance	1 inch (25 mm) diameter hail at 52 mph (23 m/s)
Appearance	Class A+
Solar Cells	96 Monocrystalline Maxeon Gen III
Tempered Glass	High-transmission tempered anti-reflective
Junction Box	IP-65, MC4 compatible
Weight	41 lbs (18.6 kg)
Max. Load	G5 Frame: Wind: 62 psf, 3000 Pa front & back Snow: 125 psf, 6000 Pa front G3 Frame: Wind: 50 psf, 2400 Pa front & back Snow: 112 psf, 5400 Pa front
Frame	Class 1 black anodized (highest AAMA rating)

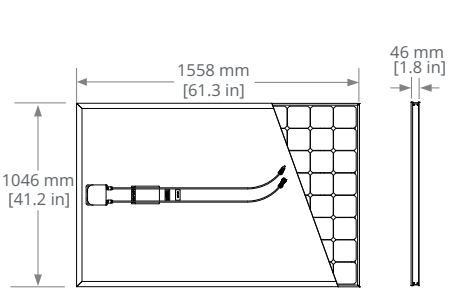

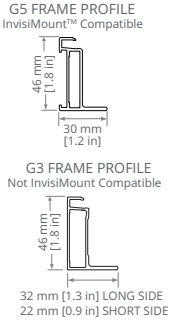

REFERENCES:
1 All comparisons are SPR-X21-345 vs. a representative conventional panel: 250 W, approx. 1.6 m², 15.3% efficiency.
2 Typically 8–10% more energy per watt, BEW/DNV Engineering "SunPower Yield Report," Jan 2013.
3 SunPower 0.25%/yr degradation vs. 1.0%/yr conv. panel. Campeau, Z. et al. "SunPower Module Degradation Rate," SunPower white paper, Feb 2013; Jordan, Dirk "SunPower Test Report," NREL, Q1-2015.
4 "SunPower Module 40-Year Useful Life" SunPower white paper, May 2015. Useful life is 99 out of 100 panels operating at more than 70% of rated power.
5 Highest of over 3,200 silicon solar panels, Photon Module Survey, Feb 2014.
6 1% more energy than E-Series panels, 8% more energy than the average of the top 10 panel companies tested in 2012 (151 panels, 102 companies), Photon International, Feb 2013.
7 Compared with the top 15 manufacturers. SunPower Warranty Review, May 2015.
8 Some restrictions and exclusions may apply. See warranty for details.
9 X-Series same as E-Series, 5 of top 8 panel manufacturers tested in 2013 report, 3 additional panels in 2014. Ferrara, C., et al. "Fraunhofer PV Durability Initiative for Solar Modules: Part 2". Photovoltaics International, 2014.
10 Compared with the non-stress-tested control panel. X-Series same as E-Series, tested in Atlas 25+ Durability test report, Feb 2013.
11 Standard Test Conditions (1000 W/m² irradiance, AM 1.5, 25° C). NREL calibration Standard: SOMS current, LACCS FF and Voltage.
12 Based on average of measured power values during production.
13 Type 2 fire rating per UL1703:2013, Class C fire rating per UL1703:2002.
14 See salesperson for details.

See www.sunpower.com/facts for more reference information.
For more details, see extended datasheet: www.sunpower.com/datasheets.

G5 frames have no mounting holes. Please read the safety and installation guide.

Document # 504828 Rev F /LTR_US

SUNPOWER®

ANNEX III: PÈRDUES TÈRMIQUES DEL TUB RECEPTOR

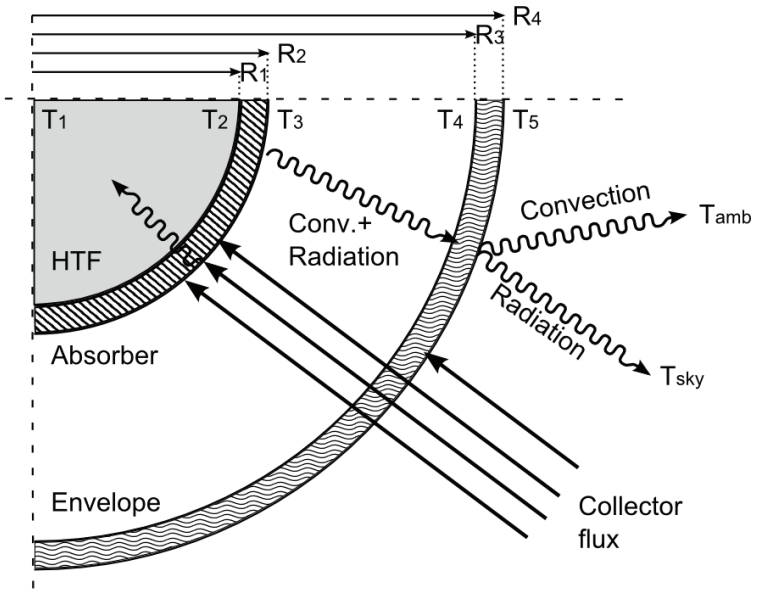

Figure 9: A heat balance for the modeled receiver. Heat transfer in the radial direction (left to right) is considered, while circumferential and axial transfer is not.

Concentrated irradiative flux from the collector passes through the transparent glass envelope (R_{3-4}), and a portion of that flux is absorbed by the glass. The absorbed flux is determined from the absorption fraction specified by the user as Envelope Absorptance (α_{env}) on the Receivers page and influences the calculated temperature of the glass. The flux that passes through the glass envelope reaches the absorber tube at R_2. Note that the fraction of energy passing through the glass envelope is specified by the Envelope Transmittance value on the Receivers page, and need not equal the compliment of the absorptance value. This is because absorptance by the glass is only one of several possible loss mechanisms. Others include reflective loss and light refraction where incoming rays are bent away from the absorber.

During operation, the heated surface at R_2 drives thermal energy through the absorber wall (R_{1-2}) and into the cooler HTF. Thermal losses from the absorber surface occur via convection and radiation exchange with the glass envelope. The glass envelope is in turn exposed to ambient air. Figure 10 shows the heat transfer network, conceptualized as a set of thermal resistances in series and parallel. This is analogous to an electrical resistance network where thermal energy represents current, thermal resistance represents electrical resistance, and temperature drop is equivalent to voltage drop. Incidentally, the same resistance formulae apply to thermal and electrical networks.

2.4.1 Modeling approach

The nodal nature of the collector loop was discussed in Section 2.1 (see Figure 2 on page 8). To summarize, each node corresponds to an assembly of individual receiver elements and collector modules. As HTF passes through the loop, it gradually warms until it reaches the design-point field outlet temperature at the end of the last SCA. The gradual warming of HTF over the length of the loop corresponds to a trend of decreasing thermal efficiency, since

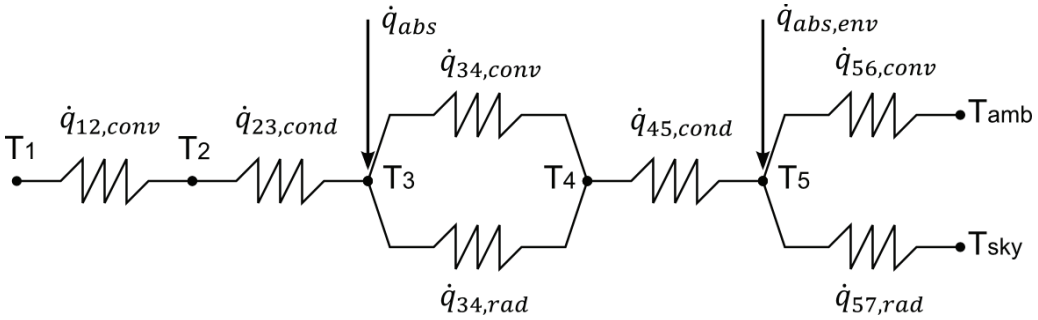

Figure 10: The thermal resistance network for the "intact" receiver model shown in Figure 9. Energy is absorbed at T_3 and T_{4-5}.

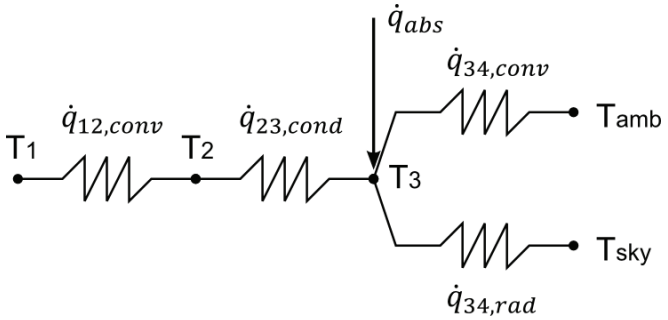

Figure 11: The thermal resistance network for the "broken glass" receiver model. Energy is absorbed on the absorber tube surface at T_3 and heat is exchanged directly with the sky and ambient temperatures.

receiver performance is inversely related to receiver temperature. Variability in receiver performance within a loop can be significant, so the receiver model is applied individually for each node in the loop. This system is solved iteratively to determine the mass flow rate that is required to meet the design outlet temperature, as discussed in Section 2.2.

The receiver model uses information about the HTF temperature, receiver geometry, ambient conditions, and incoming solar flux to determine the performance of the receiver. Conceptually, the solar field can be dissected into four different models:

1. the collector model
2. the receiver model
3. the piping model, and
4. the HTF model.

This distinction is particularly noteworthy for the receiver and HTF models. The HTF model calculates the HTF temperature throughout the loop based on absorbed energy and mass flow rate. The receiver model calculates the thermal performance of the receiver given an HTF temperature and other information. Thus, from the perspective of the receiver model, the HTF

temperature (T_1) is an input value even though T_1 is closely tied to the results calculated by the receiver model. Other specified values for the model are summarized in Table 5.

Table 5: Inputs to the receiver model

Item	Description
T_1	HTF inlet temperature
$\dot{m}_{htf}$	HTF mass flow rate
T_{amb}	Ambient temperature
T_{sky}	Effective sky temperature
v_{wind}	Wind velocity at the receiver surface
p_{amb}	Ambient pressure
$\dot{q}_{inc,i}$	Incident radiation at node i
A_{cs}	Cross-sectional area of the absorber tube
D_2	Absorber tube internal diameter
D_3	Absorber tube external diameter
D_4	Glass envelope internal diameter
D_5	Glass envelope external diameter
D_p	Internal flow plug diameter
ε_3	Absorber surface emittance
ε_4	Glass surface emittance
α_{abs}	Absorber surface absorptance
α_{env}	Glass envelope absorptance
$\eta_{col,i}$	Collector optical efficiency at node i
τ_{env}	Glass envelope transmittance
P_a	Annulus pressure
-	Annulus gas type
-	HTF type
-	Absorber material

For any solver using successive substitution, initial guess values must also be provided. The guess values for the receiver model are initially calculated based on the HTF temperature provided to the model, and depend on the condition of the receiver envelope. Temperature guesses for the absorber tube and glass envelope must be provided. Eq.[2.46] shows the initial settings for the temperatures for intact receivers, and Eq.[2.47] shows the settings for receivers with broken glass.

$$\begin{aligned} T_2 &= T_1 + 2^\circ C \\ T_3 &= T_2 + 5^\circ C \\ T_4 &= T_3 - 0.8 \cdot (T_3 - T_{amb}) \\ T_5 &= T_4 - 2^\circ C \end{aligned} \tag{2.46}$$

$$\begin{aligned} T_2 &= T_1 + 2^\circ C \\ T_3 &= T_2 + 5^\circ C \\ T_5 &= T_4 = T_{amb} \end{aligned} \tag{2.47}$$

Once guess values have been calculated, subsequent calls to the subroutine use the converged values from the previous call as the new guess values. However, several conditions may trigger recalculation of the guess values using Eq.'s[2.46] and [2.47]:

- The difference between the last T_1 and the current T_1 is greater than $50°C$
- The minimum value in the group T_{1-5} is less than the current T_{sky} value
- Any temperature from the last call returned as invalid (Not a Number error)

2.4.2 Model formulation

The first step in determining receiver heat loss is to calculate the thermal resistance between the outer absorber tube and the inner glass envelope surfaces. Both convection and radiation contribute to the total heat transfer, though convection between the two surfaces is very small for intact receivers. Convection becomes significant in cases where the vacuum is lost due to broken glass or where hydrogen from the HTF has diffused through the absorber tube wall into the annulus.

Convection from the absorber

Convection may occur either between the absorber and the inner glass surface or directly to the ambient air in the case that the envelope is broken. The convection subroutine handles both situations. First, for **intact receivers**, the annulus gas properties are evaluated at the average temperature T_{34}. Convection from R_3 to R_4 can be generally expressed in terms of thermal resistance $\hat{R}_{34,conv}$ as[7]:

$$\dot{q}_{34,conv} = \frac{T_3 - T_4}{\hat{R}_{34,conv}} \tag{2.48}$$

Where:

$$\hat{R}_{34,conv} = \frac{1}{\gamma_{34,conv}\,\pi\,D_3}$$

The receiver model calculates natural internal convection using the modified Raithby and Hollands correlation [2] (for more information on the convective algorithms, see [8] pages 11-14). The calculation for annular natural convection begins with determining the Rayleigh number at diameter D_3 using Eq.[2.49].

$$Ra_{D3} = \frac{g\,\beta_{34}\,|T_3 - T_4|\,D_3^3}{\alpha_{34}\,\nu_{34}} \tag{2.49}$$

The volumetric expansion coefficient β_{34}, the thermal diffusivity constant α_{34}, and the kinematic viscosity ν_{34} of the annular gas are all evaluated at the averaged temperature T_{34}.

[7] The subscript "34" (or other two-number subscripts in this section) denote properties, temperatures, or other quantities that describe the intermediate step between surface 3 and surface 4 in the resistance model. In practical terms, "34" can be thought of as the subscript that denotes the thermal interaction of surface 3 and surface 4. This model describes the continuous substance between surfaces 3 and 4 using thermal properties that are evaluated at the average of T_3 and T_4 (T_{34}).

Using Prandlt number $Pr_{34} = \nu_{34}/\alpha_{34}$, we calculate the heat transfer due to natural convection in the annulus and the associated heat transfer coefficient.

$$\dot{q}_{34,conv} = 2.425\, k_{34}\, \frac{T_3 - T_4}{\left(1 + \frac{D_3}{D_4}^{0.6}\right)^{1.25}} \left(\frac{Pr_{34} Ra_{D3}}{0.861 + Pr_{34}}\right)^{0.25} \tag{2.50}$$

$$\gamma_{34,conv} = \frac{\dot{q}_{34,conv}}{\pi\, D_3\, (T_3 - T_4)} \tag{2.51}$$

For very low annular pressures, the molecular density drops below the physical limit for establishing convective currents; instead, free molecular heat transfer relationships more appropriately describe convective heat loss. The receiver model handles this by using the largest convective loss predicted by either annular natural convection or free molecular heat transfer. Eq.[2.52] shows the steps for calculating free molecular heat transfer.

$$\begin{aligned} \Lambda &= C_1 \times 10^{-20} \cdot \frac{T_{34}}{P_a \cdot \zeta^2} \\ \Gamma &= \frac{c_{p,34}}{c_{v,34}} \\ b &= \frac{9\Gamma - 5}{2\Gamma + 2} \\ \gamma_{34,conv} &= \frac{k_{34}}{\frac{D_3}{2}\log\left(\frac{D_4}{D_3}\right) + \frac{b\,\Lambda}{100}\left(\frac{D_3}{D_4} + 1\right)} \\ \dot{q}_{34,conv} &= \pi\, D_3\, \gamma_{34,conv}\, (T_3 - T_4) \end{aligned} \tag{2.52}$$

In the calculation for Λ, C_1 is a constant $2.331 \times 10^{-20} \frac{mmHg \cdot cm^3}{K}$, ζ is the free-molecular collision distance shown in Table 6 [8], and P_a is the annulus pressure in $torr$.

Table 6: Values of the mean free path between collisions of a molecule for free molecular convection

Annulus Gas	ζ [cm]
Air	3.53×10^{-8}
Hydrogen	2.4×10^{-8}
Argon	3.8×10^{-8}

The annular convection calculations assume that the receiver's glass envelope is intact. However, the glass envelope sometimes breaks due to impact or excessive thermal cycling. Thermal loss from a **broken-glass receiver** is significantly higher than for an intact receiver, and the loss must be modeled differently. System Advisor provides specialized calculations for broken-glass receivers and further divides the heat transfer relationships applied based on ambient wind speed.

If the ambient wind speed is very low (less than 0.1 m/s), then the Nusselt number is calculated using the Churchill & Chu correlation for a long isothermal horizontal cylinder [13], where the fluid properties are determined at the averaged temperature T_{36}.

$$\overline{Nu} = \left[\frac{0.60 + 0.387 \cdot Ra_{D3}^{0.1667}}{\left(1 + \left(\frac{0.559}{Pr_{36}}\right)^{0.5625}\right)^{0.2963}} \right]^2 \tag{2.53}$$

The convection coefficient calculated in Eq.[2.54] is then used to determine the total convective heat transfer.

$$\begin{aligned} \gamma_{34,conv} &= \overline{Nu}\,\frac{k_{36}}{D_3} \\ \dot{q}_{34,conv} &= \gamma_{34,conv}\,\pi\,D_3\,(T_3 - T_6) \end{aligned} \tag{2.54}$$

If the ambient wind speed is above 0.1 m/s, thermal properties are required for both the air in contact with the absorber surface at T_3 and the ambient air at T_6. In this case, the Nusselt number is calculated using Zhukauskas' correlation for external forced convection [13].

$$\overline{Nu} = C\,Re_{D3}^{m}\,Pr_6^{n}\left(\frac{Pr_6}{Pr_3}\right)^{0.25} \tag{2.55}$$

Where:

$$Re_{D3} = \frac{v_6\,D_3}{\nu_6}$$

The coefficients m, n, and C are selected according to the Prandtl number and the Reynolds number as shown in Table 7. For $Pr \leq 10$, $n = .37$, otherwise $n = .36$.

Table 7: Selection of coefficients C and m for Zhukauskas' correlation based on the Reynolds number at D_3.

Reynolds Number Range					C	m
0	$\leq$	Re_{D3}	$<$	40	0.75	0.4
40	$\leq$	Re_{D3}	$<$	1000	0.51	0.5
1000	$\leq$	Re_{D3}	$<$	2×10^5	0.26	0.6
2×10^5	$\leq$	Re_{D3}	$<$	10^6	0.076	0.7

To summarize the absorber convection calculations:

1. Convection loss is determined based on the condition of the receiver (whether the glass envelope is intact or broken).

2. If the glass is intact, the natural convection coefficient and the molecular diffusion convection coefficient are both calculated and compared, with the larger of the two selected for use in the loss equation.

3. If the envelope is not intact, direct convection to ambient is calculated based on whether the wind speed is below or above 0.1 m/s.

No matter the method used to calculate the convective loss coefficient from the absorber, the thermal resistance due to convection is expressed as follows.

$$\hat{R}_{34,conv} = \frac{1}{\gamma_{34,conv}\,\pi\,D_3} \tag{2.56}$$

Radiation from the absorber

Radiation loss from the absorber tube to the surroundings is the most significant contributor to heat loss for intact collectors. Two alternate equations are used for calculating radiative loss depending on whether the glass envelope is intact. For **intact receivers**, radiative exchange is between the absorber surface at D_3 and the inner envelope surface at D_4, as shown in Eq.[2.57].

$$\begin{aligned} \gamma_{34,rad} &= \sigma(T_3^2 + T_4^2)\,\frac{T_3 + T_4}{\frac{1}{\varepsilon_3} + \frac{D_3}{D_4}\left(\frac{1}{\varepsilon_4} - 1\right)} \\ \dot{q}_{34,rad} &= \pi\,D_3\,\gamma_{34,rad}\,(T_3 - T_4) \end{aligned} \tag{2.57}$$

If the receiver **envelope is broken**, radiation exchange occurs directly between the absorber surface and the ambient surroundings at temperature T_{sky}.

$$\dot{q}_{34,rad} = \sigma\,\gamma_{34,rad}\,\varepsilon_3\,\pi\,D_3\,(T_3^4 - T_{sky}^4) \tag{2.58}$$

Where:

$$\gamma_{34,rad} = \frac{\dot{q}_{34,rad}}{\pi\,D_3\,(T_3 - T_7)}$$

The radiation thermal resistance $\hat{R}_{34,conv}$ is calculated with the same arrangement used in Eq.[2.56] above. The total thermal resistance between the absorber surface and the glass envelope is expressed as two parallel thermal resistances and applies only for intact receivers.

$$\hat{R}_{34,tot} = \left(\frac{1}{\hat{R}_{34,conv}} + \frac{1}{\hat{R}_{34,rad}}\right)^{-1} \tag{2.59}$$

Conduction across the glass envelope

Conduction across the intact glass envelope is modeled using the formula for radial resistance in a cylinder [17], assuming the thermal conductance $k_{45} = 1.04 \frac{W}{m-K}$.

$$\hat{R}_{45,cond} = \frac{\log\left(\frac{D_5}{D_4}\right)}{2\pi k_{45}} \tag{2.60}$$

Convection and radiation loss from the envelope

Like convection from the absorber to ambient air in the case of broken glass receivers, convection loss from the glass envelope occurs between a cylindrical object and free-stream air. Thus, the equations developed for convective loss from broken receivers can be reused here. For wind speeds of less than 0.1 m/s, the Churchill and Chu correlation in Eqs.[2.53-2.54] is used, otherwise Eq.[2.55] is used. Air properties are evaluated at T_5 and T_6 rather than at T_3 and T_6.

Radiative loss is calculated using Eq.[2.58], substituting T_5 for T_3. The corresponding thermal resistances are:

$$\hat{R}_{56,conv} = \frac{1}{\gamma_{56,conv}\,\pi\,D_5} \tag{2.61}$$

$$\hat{R}_{57,rad} = \frac{1}{\gamma_{57,rad}\,\pi\,D_5} \tag{2.62}$$

Heat flows and temperatures

Thermal energy is absorbed into the resistance network at two locations, as illustrated in Figure 10 above. The absorber tube receives most of the thermal energy incident on the receiver at D_3, but a small portion of the incoming energy is also absorbed in the glass envelope at D_5. The energy absorbed by absorber tube i is a function of the energy concentrated by the collector $\dot{q}_{inc,i}$, the envelope transmittance τ_{env}, and the absorber surface absorptance α_{abs}.

$$\dot{q}_{abs,i} = \dot{q}_{inc,i}\,\eta_{opt,i}\,\tau_{env}\,\alpha_{abs} \tag{2.63}$$

The energy absorbed by the envelope is:

$$\dot{q}_{abs,env,i} = \dot{q}_{inc,i}\,\eta_{opt,i}\,\alpha_{env} \tag{2.64}$$

We estimate the heat transfer from the absorber surface to the inner envelope surface using the temperature guess values in Eq.[2.46] for T_3 and T_4. This heat flow ($\dot{q}_{34,tot}$) is increased by the energy absorbed within the envelope. For simplicity, the energy is assumed to be absorbed just after the inner envelope wall between D_4 and D_5 so that the thermal energy must travel the entire distance between the envelope walls. Thus, the thermal energy conducted across the

wall is expressed as:

$$\dot{q}_{45,cond} = \dot{q}_{34,tot} + \dot{q}_{abs,env} \tag{2.65}$$

The outer envelope surface temperature is then the inner surface temperature minus the heat flow conducted scaled by the thermal resistance.

$$T_5 = T_4 - \dot{q}_{45,cond}\, \hat{R}_{45,cond} \tag{2.66}$$

Thermal losses from the envelope to ambient are now redetermined for this iteration with the newly recalculated glass envelope outer surface temperature T_5.

$$\begin{aligned} \dot{q}_{56,conv} &= \frac{T_5 - T_{amb}}{\hat{R}_{56,conv}} \\ \dot{q}_{57,rad} &= \frac{T_5 - T_{sky}}{\hat{R}_{57,rad}} \end{aligned} \tag{2.67}$$

This fully defines the thermal resistance network from the outer absorber surface to the surroundings. If we consider the temperature profile of an intact receiver during operation, the figurative "top of the temperature hill" is located at the boundary between the absorber surface and the inner annulus (D_3). Heat always flows "downhill"; assuming we know the temperature at D_3, we can now recalculate the magnitude of the heat flow from the absorber to ambient. This quantity defines the receiver heat loss. This can be done analytically by expressing the total heat loss in terms of the equivalent thermal resistance between D_3 and ambient, and the total temperature difference between T_3 and the ambient temperatures T_{amb} and T_{sky}. The heat conducted across the glass envelope is equal to the heat flow across the annulus ($\dot{q}_{34,tot}$) plus the heat absorbed directly by the envelope. This total heat flow is then radiated/convected to ambient, though the practical receiver heat loss is only equal to the heat transferred away from the absorber tube across the annulus, and the envelope energy absorption is accounted for an an optical loss. Thus:

$$\dot{q}_{hl} = \dot{q}_{34,tot} = \dot{q}_{45,cond} = \left(\dot{q}_{56,conv} + \dot{q}_{57,rad} - \dot{q}_{abs,env}\right) = \frac{\Delta T_{hl}}{\hat{R}_{3,amb}} \tag{2.68}$$

A practical implementation of this equation is easily derived by applying resistance network rules to the section of Figure 10 between T_3 and the ambient temperatures. Eq.[2.68] is then equivalently:

$$\dot{q}_{hl} = \frac{(T_3 - T_{amb})\, \hat{R}_{57,rad} + (T_3 - T_{sky})\, \hat{R}_{56,conv} - \dot{q}_{abs,env}\, \Omega_{\hat{R}}}{\hat{R}_{34,tot}\, \hat{R}_{57,rad} + \hat{R}_{34,tot}\, \hat{R}_{56,conv} + \Omega_{\hat{R}}} \tag{2.69}$$

Where:

$$\Omega_{\hat{R}} = \hat{R}_{56,conv}\,\hat{R}_{57,rad} + \hat{R}_{45,cond}\,\hat{R}_{57,rad} + \hat{R}_{45,cond}\,\hat{R}_{56,conv}$$

This equation is somewhat simplified as the envelope resistances drop out in the case that the receiver glass is removed and the absorber surface is in direct thermal communication with the ambient.

$$\dot{q}_{hl} = (T_3 - T_6)\,\hat{R}_{34,conv} + (T_3 - T_7)\,\hat{R}_{34,rad} \tag{2.70}$$

Having considered convective and radiative losses from the receiver for both intact and broken receivers, one remaining heat loss mechanism must be accounted for. This is conductive loss from the support brackets in contact with the receiver ends. Radiation and convection heat losses tend to overwhelm bracket conduction heat loss, so the System Advisor interface excludes inputs related to this loss. System Advisor hard-codes the required inputs for this calculation to reduce the number of user input variables. Table [8] enumerates the bracket geometry and material properties assumed by System Advisor.

Table 8: Bracket geometry and material properties assumed by System Advisor for conductive heat loss calculations

Item	Assumed Value	Units
Effective bracket perimeter	20.32	cm
Effective bracket diameter	5.08	cm
Minimum bracket cross sectional area	1.6129×10^{-4}	m^2
Conduction coefficient (carbon steel, 600K)	48.0	$\frac{W}{m-K}$
Effective bracket base temperature	$T_3 - 10$	$^{\circ}C$
Single receiver length	4.06	m

Bracket heat loss is estimated by assuming that the bracket convects heat to the surroundings at a driving temperature difference of $T_{brac} - T_{amb}$, where the average bracket temperature T_{brac} is defined as:

$$T_{brac} = \frac{1}{2}\left[\frac{T_{base} + T_{amb}}{2} + T_{amb}\right] \tag{2.71}$$

The base temperature T_{base} is the effective bracket base temperature from Table 8. Like convection from the outer glass envelope, convection from the bracket is subdivided into still-air convection (velocity less than 0.1 m/s) and forced convection. The Nusselt number for natural convection is given in Eq.[2.53] as shown above, except using Rayleigh and Prandtl numbers corresponding to the average bracket temperature. The convective heat loss coefficient is then scaled by the effective bracket diameter.

$$\gamma_{brac} = \overline{Nu}_{brac}\,\frac{k_{brac}}{D_{brac}} \tag{2.72}$$

Forced convection from the bracket is calculated analogously to the procedure described in Eq.[2.55] and Table 7, but using bracket temperatures. The bracket convective heat loss calculation uses either the coefficient for forced convection or for natural convection, depending on the ambient wind speed. This coefficient γ_{brac} is used to calculate the heat loss as shown in Eq.[2.73] for a given bracket perimeter per_{brac}, cross-sectional area $A_{brac,cs}$, and single receiver length L_{rec}.

$$\dot{q}_{brac} = \sqrt{\gamma_{brac}\, per_{brac}\, k_{brac}\, A_{brac,cs}} \left(\frac{T_{base} - T_6}{L_{rec}} \right) \tag{2.73}$$

The total heat loss from the receiver is the sum of convection, radiation, and bracket conduction losses. The energy flow into the HTF $\dot{q}_{12,conv}$ is then equal to the energy absorbed by the absorber tube minus the heat loss from the receiver. The heat loss value is reduced by the amount of heat absorbed in the glass envelope that also must be rejected; this avoids double-counting the heat loss from the absorber tube.

$$\dot{q}_{12,conv} = \dot{q}_{23,cond} = \dot{q}_{abs} - \dot{q}_{hl} \tag{2.74}$$

Using the calculated value for heat flow into the HTF and the guessed average HTF temperature T_1, we calculate the temperature drop from the inner absorber tube surface to the HTF due to the internal convective resistance. The convection correlations require fluid properties evaluated at the inner wall temperature and the bulk HTF temperature, and are divided into several cases: for HTF flow velocities greater than 0.1 m/s, the Nusselt number is calculated for either annular or round-pipe flow, and for higher velocities the Nusselt number is determined using a modified Gnielinski correlation [11]. For low velocities with annular flow:

$$\begin{aligned} \overline{Nu}_{12} &= 41.402\, D_R^5 - 109.702\, D_R^4 + 104.570\, D_R^3 - 42.979\, D_R^2 \\ &\quad + 7.686\, D_R + 4.411 \end{aligned} \tag{2.75}$$

Where:

$$D_R = \frac{D_P}{D_2}$$

and for low velocities with normal pipe flow, the Nusselt number is fixed where $\overline{Nu}_{12} = 4.36$. The inner wall temperature for low-flow conditions is then:

$$T_2 = T_1 + \frac{\dot{q}_{12,conv}\, D_{hyd}}{\pi\, D_2\, k_1\, \overline{Nu}_{12}} \tag{2.76}$$

Any significant HTF velocity drives the Nusselt number sufficiently high that the inner wall temperature approaches the bulk HTF temperature. This will be the case for most situations where a minimum flow is enforced in the field during off-sun conditions.

The final step in solving the receiver model is to recalculate the absorber tube outer surface

temperature, T_3. Recall that this value was initially guessed, but now enough information is available to calculate this temperature and update the guess for iteration. T_3 is found this time as a function of the inner wall temperature T_2 and the heat flow by conduction across the tube wall.

$$T_3 = T_2 + \frac{\dot{q}_{23,cond}}{2\,\pi\,k_{23}}\,\log\frac{D_3}{D_2} \tag{2.77}$$

The calculation process beginning with Eq.[2.65] and ending with Eq.[2.77] is repeated iteratively until convergence is achieved in temperatures T_3 and T_4 with respect to their previous iteration guess values T_{3g} and T_{4g}. Convergence is obtained when the error calculated in Eq.[2.78] falls below a tolerance of 0.05 or when the number of iterations exceeds 4.[8]

$$err = \sqrt{\left(\frac{T_{4g} - T_4}{T_4}\right)^2 + \left(\frac{T_{3g} - T_3}{T_3}\right)^2} \tag{2.78}$$

Section 2.4 Summary

- The receiver model uses a 1-dimensional formulation, where heat flows uniformly in the radial direction.
- The receiver can account for a broken glass envelope, and for either air, argon, or hydrogen gas in the receiver annulus.
- The model is analogous to a thermal resistance network, with heat transfer occurring in both parallel and series flow .
- Guess values are used to iteratively solve the temperature and heat flow distribution in the receiver.
- Model convergence is achieved when temperatures T_3 and T_4 remain acceptably constant between iterations.

2.5 Piping model

The largest *parasitic* loss for a trough plant is the electricity consumed by the solar field HTF pumps. Since pumping power scales proportionally with the HTF pressure drop across the solar field and with the HTF mass flow rate, accurately capturing both of these values is important in characterizing the total plant performance. System Advisor takes a moderately detailed approach in the design and performance modeling of the solar field piping. The piping model in System Advisor is derived directly from work presented in [14].

The piping model in System Advisor accounts for the pressure drop associated with a variety of field components, including:

[8] These tolerance criteria were selected based on a sensitivity analysis that balanced model speed with annual output precision.

ANNEX IV: CORBES DE POTÈNCIA TÈRMICA I ENERGIA NETA PRODUÏDES HORÀRIES DE CADA MÉS.

- Potència tèrmica mensual sense caldera auxiliar

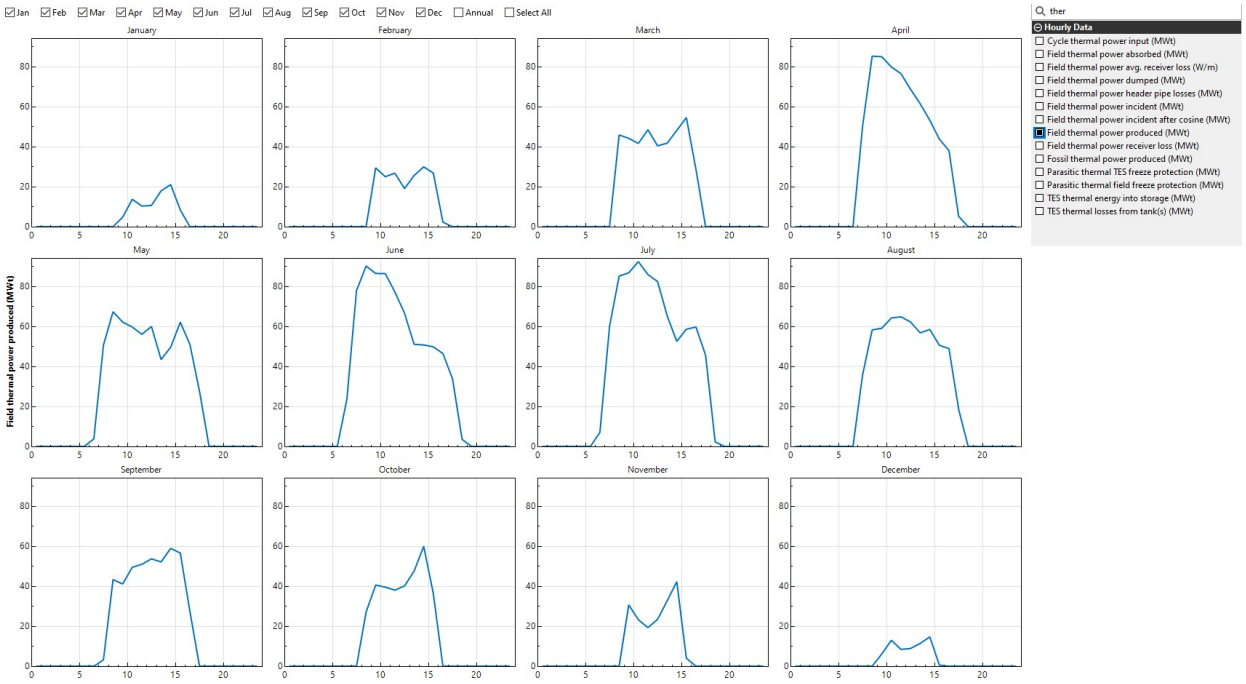

- Potència tèrmica mensual i energia neta produïda sense caldera auxiliar

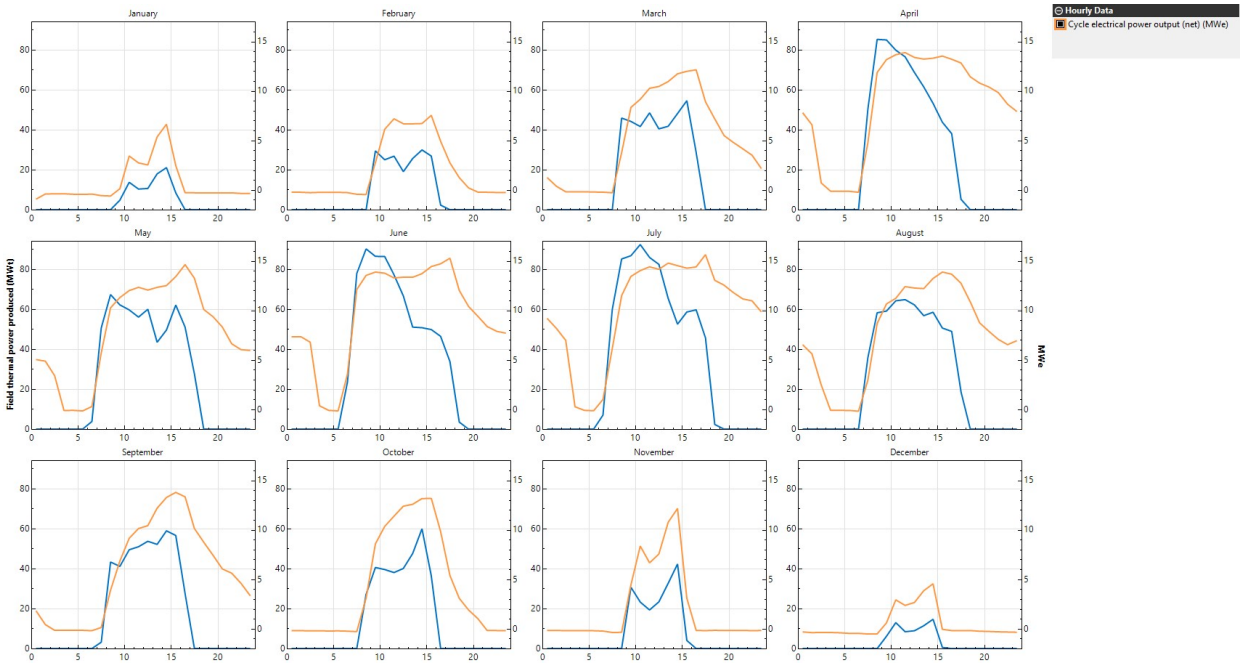

- Potència tèrmica mensual amb suport de caldera auxiliar

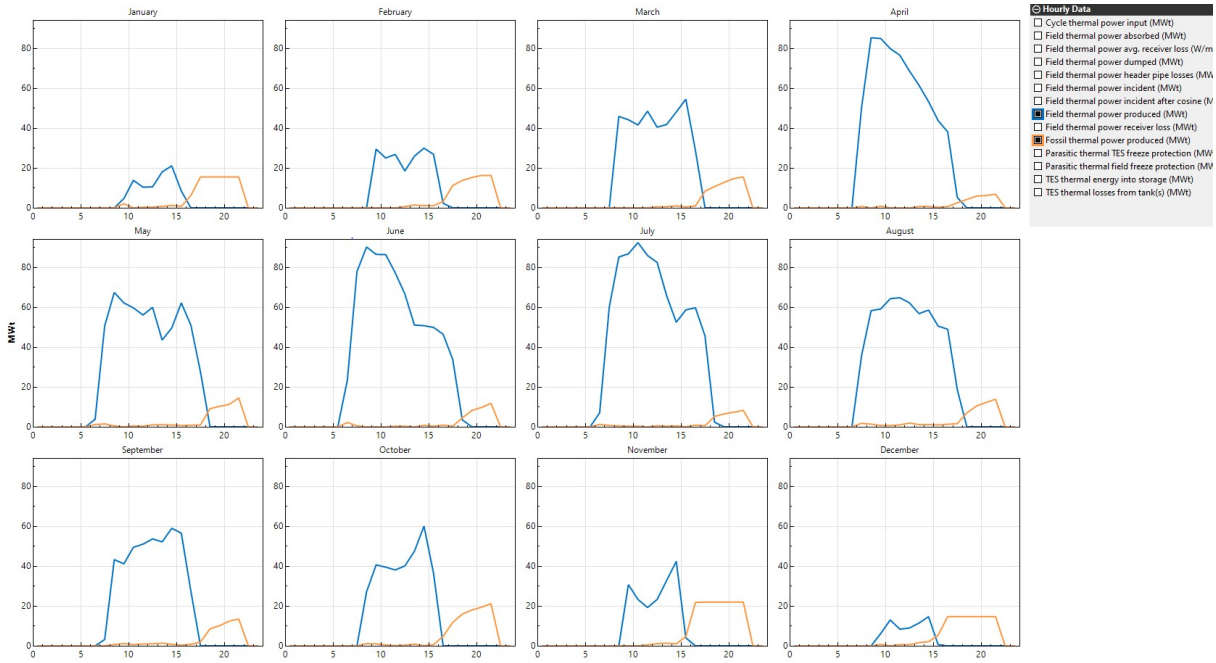

- Potència tèrmica mensual i energia neta produïda amb caldera auxiliar